Pergamon

PII: S0191-8141(97)00079-5

Journal of Structural Geology, Vol. 20, No. 1, pp. 3 to 19, 1998

0191-8141/98 $19.00 + 0.00

Lateral displacement variation and lateral tip geometry of normal faults in the Canyonlands National Park, Utah

J. A. CARTWRIGHT

Imperial College of Science, Technology and Medicine, Department of Geology, Prince Consort Road, London SW7 2BP, U.K.

and

C. S. MANSFIELD

Nederlandse Aardolie Maatschappij B.V., Schepersmaat 2, 9405 TA, Assen, The Netherlands

(*Received* 15 *November* 1996; *accepted in revised form* 15 *September* 1997)

Abstract—The along-strike displacement variation of 20 well-exposed normal faults from the Canyonlands, Utah, is described and analysed. The displacement profiles of these faults are highly variable, and most irregularities can be related to fault segmentation. Many of the profiles are highly asymmetric, and this can be related to mechanical interaction in some cases. Linear displacement tapers are observed towards all the lateral tips, but the percentage of trace length over which this linear taper occurs is highly variable. Three distinct lateral tip geometries are recognised, referred to informally as types A, B and C. Type A tips have a simple Mode III displacement geometry, Type B tips are characterised by a zone of extensional 'fissures' surrounding the fault tip, and Type C tips are characterised by the development of a monocline beyond the tip. Lateral displacement variation towards tips was analysed by measuring displacement gradients from systematic positions along the fault trace. Lateral displacement gradients measured for 39 tips exhibit a wide range of values (0.016–0.25). Fourteen of these lateral tips are regarded as 'active' since they exhibit signs of recent surface rupturing. These active tips have a similar range of lateral displacement gradients (0.019–0.25) to the overall population. Lateral displacement gradients were correlated with fault parameters such as length, length/maximum displacement (for faults and segments), and proximity to adjacent faults. No positive correlations were found. We suggest that the large range of lateral displacement gradients is mainly due to interactions between neighbouring faults. Additional complexities are likely to have resulted from strength heterogeneities related to jointing, from local variations in remote loading stresses and the frictional properties of the fault surfaces, and from processes related to segment linkage. © 1998 Elsevier Science Ltd.

INTRODUCTION

Numerous recent studies of normal faults from a variety of tectonic settings have presented displacement profiles derived from surface or sub-surface mapping (Gudmundsson, 1987a,b; Walsh and Watterson, 1990; Peacock and Sanderson, 1991; Dawers *et al.*, 1993; Trudgill and Cartwright, 1994; Dawers and Anders, 1995; Cartwright *et al.*, 1996; Schlische *et al.*, 1996). One common feature seen in these profiles is that the often irregular distributions of displacement on normal faults on contrasting scales have been attributed to fault segmentation, with substantial departures from idealised smooth displacement distributions generally occurring at relay structures. This form of irregularity has been explained by interaction between fault segments prior to segment linkage (Peacock and Sanderson, 1991).

The aim of this paper is to describe the displacement distribution measured for 20 normal faults from the Canyonlands of S.E. Utah, and discuss their displacement profiles and geometry in relation to the lateral propagation of the faults. Description and analysis of geometry and displacement distribution near the lateral tips of normal faults is an essential step towards developing conceptual models for their growth (Cowie and Scholz, 1992a). Unfortunately, relatively few areas have sufficient clarity of exposure of the tip regions of faults to permit detailed mapping and displacement profiling. The Canyonlands area is ideal for this type of study because the deformation is geologically recent (Pleistocene–Recent), and only modest erosion and deposition has occurred during the deformation. Fault displacements are therefore closely approximated by the surface topography, meaning that tip geometries and fault displacement profiles can be accurately observed for a large number of faults within the confines of a single deformational province.

GEOLOGICAL SETTING

The geological setting and structural context of the Canyonlands Grabens have been described by Lewis and Campbell (1965), McGill and Stromquist (1979), Trudgill and Cartwright (1994), Cartwright *et al.* (1995), Cartwright *et al.* (1996) and Schultz and Moore (1996). The study area is on the northwestern flank of the Monument Upwarp, a Laramide compressional structure in the Colorado Plateau (Hintze, 1988), with late Palaeozoic to early Mesozoic sedimentary rocks exposed at surface

along the anticlinal axis. An approximately 500 m thick succession of sandstones and limestones is faulted in the Needles District of the Canyonlands National Park, over an area measuring *ca* 60 km by 20 km. This faulted succession overlies a Late Carboniferous polycyclic evaporate sequence (the Paradox Formation) that is approximately several hundred metres thick in the study area (Lewis and Campbell, 1965). The faults are all normal, and are developed in an arcuate belt immediately adjacent to the deeply incised gorge of the Colorado River as it passes through Cataract Canyon (Fig. 1). The normal faulting is a gravitational response to the pronounced phase of incision of the Colorado River from the Late Pliocene to the present day (Baker, 1933; McGill and Stromquist, 1979).

DISPLACEMENT PROFILING

Definitions and nomenclature

The faults in the study area are all segmented and are organised into a densely faulted array with an average spacing of a few hundred metres (Trudgill and Cartwright, 1994). This means that many of the faults overlap with at least one neighbouring fault of a similar throw sense within a nominal separation distance of half the trace length of the fault (Fig. 1). Many of the overlap relationships exhibit soft linkage characteristics as described by Walsh and Watterson (1991), but to avoid the ambiguity implicit in any definition of a fault that includes soft-linked, overlapping segments based on a single two-dimensional representation of the geometry (Mansfield, 1996, p. 37), we prefer to define individual faults on the basis of a structurally continuous fault trace at surface. Segmented faults are thus defined to be composed entirely of hard-linked segments (Walsh and Watterson, 1991), connected at breached relay structures (Trudgill and Cartwright, 1994). Lengths of faults are defined as straight-line distances between lateral tips. Lateral tips are defined at surface as points of zero vertical displacement on fault planes.

Methodology

Approximately 150 faults were recognised in the study area from aerial photographs (USGS 1:33 000, 1981, project number GS-VFBL-F, 2-81 to 2-94). Of these, 103 were mapped in the field using 1:10 000 aerial photographic enlargements. This set of mapped faults forms the basis for compilations of displacement and length statistics for the Canyonlands fault system (Cartwright *et al.*, 1995, 1996). Maximum displacements on the mapped faults range from 1.5 m to 150 m, and their trace lengths range from 108 m to 6584 m.

Fault displacement values were surveyed along part or all of the trace length of 31 of the 103 mapped faults. Displacement was measured by correlating bedrock stratigraphy in the hangingwall with the footwall, and observing the vertical offset in a correlative marker horizon using a hand-held Abney Level (Fig. 2). Bedrock in the hangingwalls of most of the faults in the area is largely concealed by a thin cover (0–10 m) of alluvial and aeolian sediments. However, incised streams and sink holes provide frequent positions from which to establish the stratigraphic datum, and complete exposure in footwall scarps was invaluable in constraining the footwall to hangingwall stratigraphic correlations (Fig. 2).

Baseline distances were measured to an accuracy of $\pm 2\%$ from ground positions established on the enlarged aerial photographs. The combination of baseline distance error, angular separation error, uncertainty in stratigraphic correlation, and uncertainty in cover thickness resulted in a cumulative error of no more than 10% in the vertical displacement measurements. Lateral fault tips were located to within a few tens of metres using the enlarged aerial photographs. The concealment of these tips by sedimentary cover in the hangingwall (Fig. 2) introduced minor errors ($<5\%$) into measurements of fault trace length.

The sampling interval of displacement measurements was chosen to ensure that any lateral variations in the local displacement gradient would be accurately recorded. Due to the complete exposure of footwall bedding in the fault scarps, many lateral variations in local gradients could be identified from inflections in footwall bedding. Hangingwall contributions to lateral displacement variation could be identified with lesser precision from gradient changes in the surface topography in the hangingwalls. Sampling density was highest in the vicinity of relay structures and close to lateral tips. Importantly, the first displacement measurement along any given fault from its tip was consistently sited at the point where the displacement from that point to the tip could be clearly identified as having a linear taper, i.e. there were no visible changes of gradient in the hangingwall sedimentary cover nor in the footwall bedding.

Displacement profiles

Displacement profiles were surveyed along the complete trace length of 20 faults, and the resulting displacement–distance (d–x) profiles are presented in Fig. 3. An additional 11 faults were surveyed over approximately half of their trace lengths, and a further 22 faults were only surveyed in the region close to the tip.

The d–x profiles exhibit a range of forms including simple and symmetric (e.g. fault 213), flattish-topped with steep margins (faults 10 and 13) and irregular and strongly asymmetric (e.g. faults 8, 17 and 44). Comparisons with idealised displacement profiles (e.g. 'C' and 'M' types of Peacock and Sanderson, 1991) are therefore difficult, and the variability means that simple end member types are not discernible as such. It is clear from Fig. 3, however, that the shortest faults have simpler profiles than the longer faults. This could be interpreted

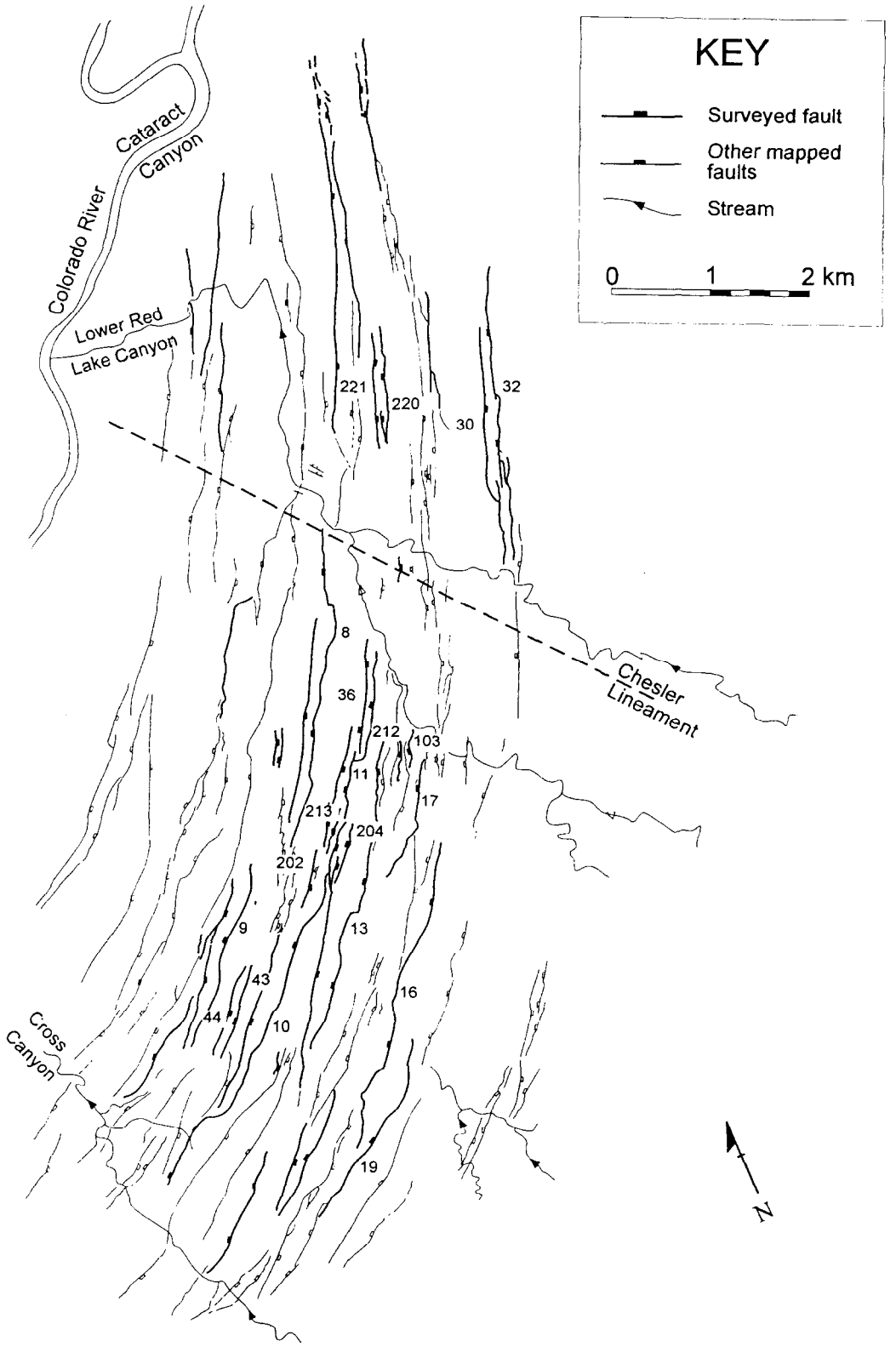

Fig. 1. Map of the study area showing the distribution of mapped and surveyed normal faults (numbered). Numbers of faults are referred to in the text and in other figures. For location of study area, see Cartwright *et al.*, 1995, their fig. 1. The Chesler Lineament is an inferred basement structure (McGill and Stromquist, 1979).

as resulting from some dimensional parameter influencing the displacement geometry (Dawers *et al.*, 1993). Alternatively, it may simply be a resolution artefact resulting from the disproportionately higher cover sediment thickness to displacement ratio for small faults in comparison to large faults.

Many faults in the study area developed as one of a pair of graben-bounding structures (McGill and Strom-

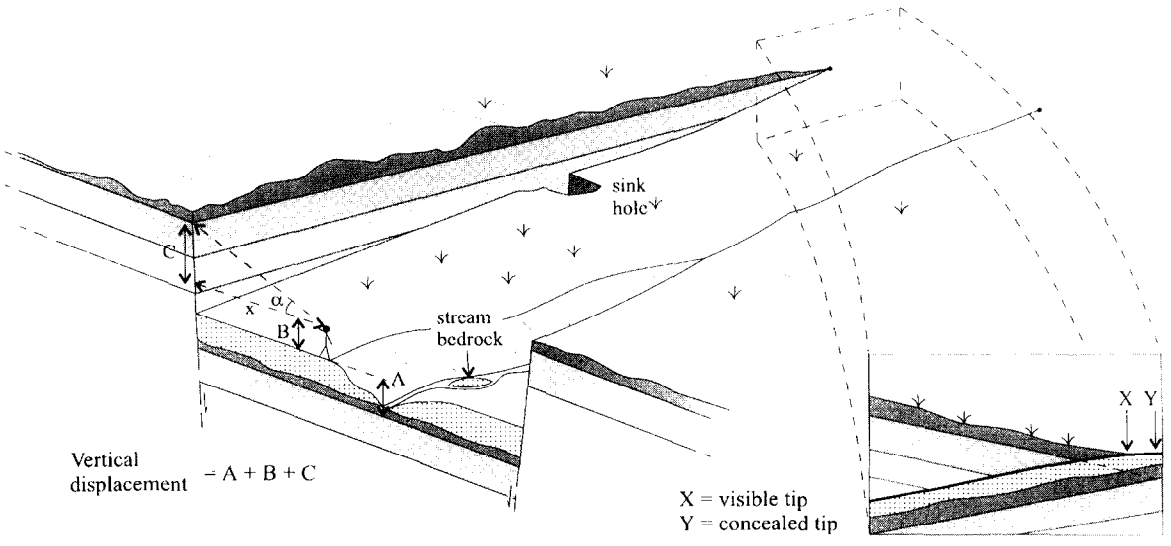

Fig. 2. Schematic diagram showing the method used to survey the vertical displacement on faults in the study area. The hand-held Abney level is used to calculate C, B is fixed, and A is estimated from bedrock exposures in the hangingwall. The inset diagram shows the difference between the tip position at surface, and the true tip position concealed beneath the surficial sediment cover (light stipple).

quist, 1979). Six of these pairs of graben-bounding faults were surveyed (Fig. 1). In some cases the displacement variation on one graben-bounding fault is similar in position and magnitude to that defining the opposite margin of the graben, with similar degrees of asymmetry (e.g. faults 221 and 220). In other cases the displacement patterns are completely different on either side of a single graben (e.g. faults 11 and 36). It is evident, therefore, that the growth of graben-bounding pairs of faults is not always coupled in such a way as to maintain complementary displacement profiles.

The grossly asymmetric shape of some of the multi-segment faults is one of the most interesting features of the displacement profiles. This asymmetry does not appear to be related to regional boundary conditions since there is no systematic orientation for the direction of skewness of displacement profiles, i.e. the displacement maximum is neither consistently to the NE nor the SW of the mid-point of asymmetric fault profiles. Asymmetry in displacement profiles is more typically associated with displacement profiles of individual segments along either a soft or hard-linked segmented fault, where interaction between segments prior to linkage results in accentuation of displacement gradients in the region of segment overlap (Walsh and Watterson, 1990; Peacock and Sanderson, 1991; Huggins *et al.*, 1995). Some of the more highly asymmetric profiles (e.g. faults 8 and 17) are candidates for this type of interaction effect since they approach to within a short distance (relative to their trace lengths) of neighbouring faults at their respective steeper tapering tips (Fig. 1). However, some relatively isolated faults also have asymmetric profiles (e.g. faults 220 and 221, Figs 1 & 3), so it is evident that proximity to nearest overlapping faults is not the only factor influencing the development of asymmetric profiles. A simple analysis of the degree of asymmetry of individual faults relative to the distance to the nearest fault or fault tip revealed no systematic relationship, possibly because the density of the fault network means that there are multiple opportunities for interaction between overlapping faults within relatively short distances (compared to trace lengths).

All the mapped faults in the study area exhibit a segmented trace geometry in map view, i.e. individual faults can be divided into component segments based on offsets, overlaps, or abrupt changes in strike (Cartwright *et al.*, 1995, 1996). This segmented geometry can be seen in most of the displacement profiles in Fig. 3 as irregular distributions of displacement along strike, with boundaries between adjacent segments marked either by substantial displacement minima or by splay faults (c.f. Huggins *et al.*, 1995). The 'summed' displacement profile (displacement on the main fault plus any synthetic splay faults) produces a smoother profile than that of the main fault alone (Fig. 3). Breached relay structures are recognisable as splay faults with triangular displacement profiles (e.g. centre of fault 8). The triangular taper of displacement on these splay faults is a close approximation to the displacement gradient of the relay ramp at the time of breaching (Cartwright *et al.*, 1996, their fig. 10).

Displacement profiles of individual segments within the segmented faults are commonly asymmetric, with the steepest displacement gradients at relay structures (Trudgill and Cartwright, 1994). This asymmetry of individual segments is not systematically related to the overall profile of the segmented fault. Faults whose overall profiles are either symmetric or asymmetric have component segments that can be a mixture of symmetric and asymmetric profile types. Asymmetry of overlapping segments is strong evidence for mechanical interaction

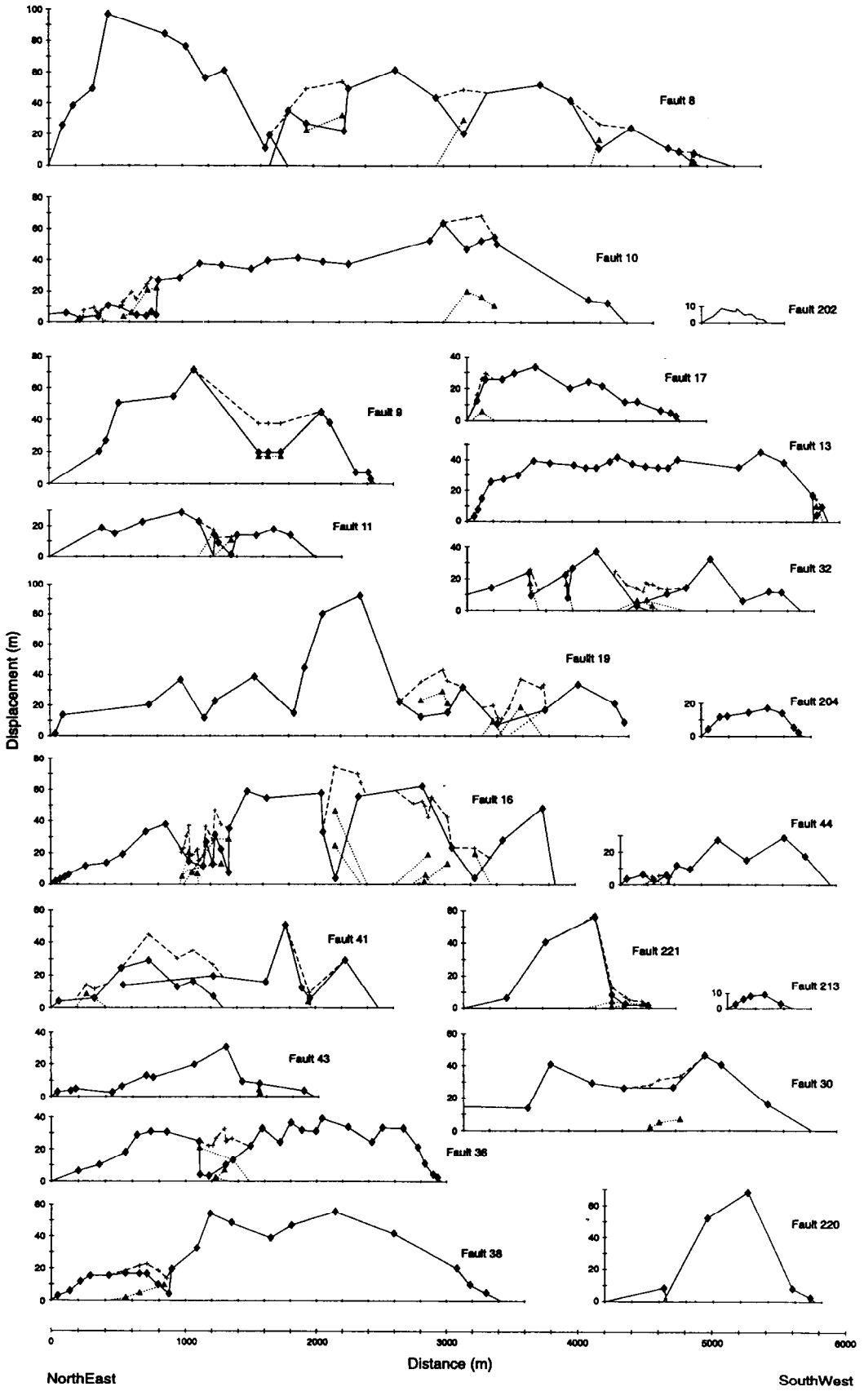

Fig. 3. Displacement profiles of 20 surveyed faults from the study area (located in Fig. 1). Scales are uniform for all the profiles. Solid lines are profiles of main faults, dotted lines are profiles of splays at relay structures, and dashed lines are summed displacement profiles (splays and main faults). Errors in displacement values are $< 10\%$. Positioning accuracy is approximately 10 m.

prior to linkage (Walsh and Watterson, 1990; Peacock and Sanderson, 1991).

There is no systematic distribution for the length of segments on any given fault. For example, the longest segments do not always occur in the central portions of a fault, with a general reduction in length of segments towards the lateral fault tips. Nor is there any systematic position for the segment with the largest displacement. Some faults have their maximum displacement on the central segment (e.g. fault 10) others on an external segment (e.g. fault 8). This complex distribution of segments is thought to be the result of a fault growth history involving the lateral propagation and linkage of precursor segments where length distributions of segments in a segmented and linked fault are influenced by nucleation positions and alignments prior to linkage (Cartwright *et al.*, 1995, 1996).

The shape and 'taper' of the displacement profiles from the maximum displacement position on the fault to the lateral tips is highly variable. In some cases the shape is approximately linear, (e.g. southwestern portion of fault 10), in others the maximum displacement position is separated from the tips by several maxima and minima (e.g. fault 19). The shape of the displacement profiles from the maximum displacement position on the outermost segments is also variable. In many cases the shape is almost a linear taper (e.g. faults 8, 10, 16, 17, 30 and 38), in some cases the profile shape is stepped with an often pronounced 'shoulder' (e.g. faults 13 and 41), and in others (e.g. faults 9 and 38) there is a gentle inflection with a concave shape reminiscent of the 'bell-shaped' profile of Cowie and Scholz (1992a). Some of these shapes are undoubtedly distorted by measurement error and sampling limitations, but the variability is too large to be attributed entirely to these effects. The significance of this variability is considered later (see Lateral Displacement Variation Towards Lateral Tips).

LATERAL TIP GEOMETRY

Three recurring types of lateral tip with distinctive geometries are recognised from structural mapping and displacement surveying (Fig. 4). These three types of tip geometry are described below, and the significance of the geometry and minor associated structures for the fault propagation history is considered later (see Discussion). The distribution of the three types of tip is shown in Fig. 5. This map shows that there is no specific combination of tip types for particular faults. Some faults have similar types at both lateral tips (A–A, B–B, C–C), others different combinations (A–B, A–C, B–C). It should be noted that the subdivision into the three types is purely for analytical purposes in this study, and no formal nomenclature is implied by the classification and description.

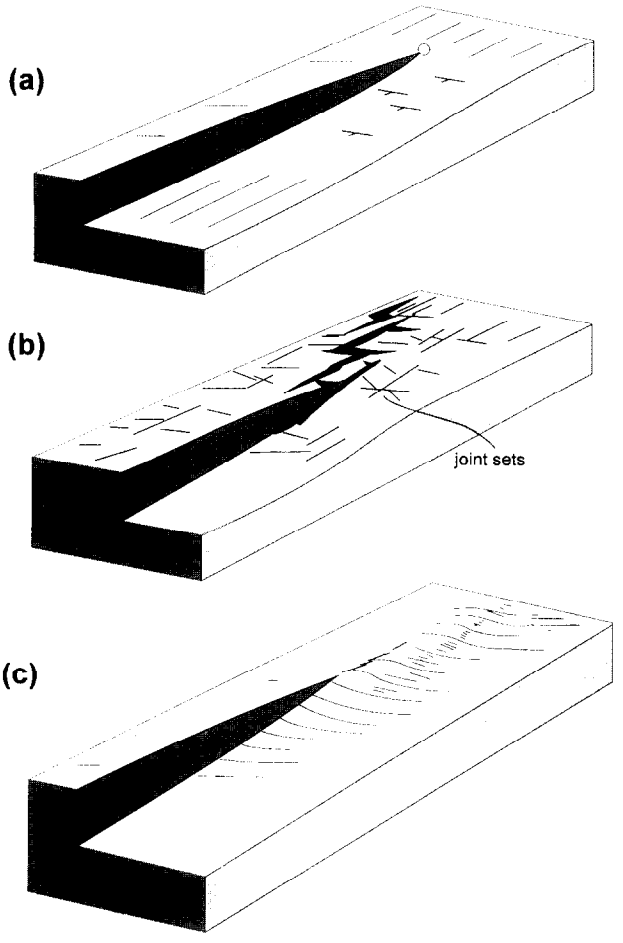

Fig. 4. Synoptic structural block diagrams showing the main features associated with the three types (A, B, and C) of lateral tip distinguished in the Canyonlands.

Type A tips (Fig. 4a)

This is the most common of the three types of tip, and is characterised by a simple tapering of displacement on the main fault with no substantial complementary fracturing or folding adjacent to the fault. Bedding strike is approximately orthogonal to fault strike in the region approaching the tip in both footwall and hangingwall. There is no recognisable zone of localised deformation beyond the tip, i.e. no obvious process zone, but in some cases this may be concealed beneath the sedimentary cover.

Type B tips (Fig. 4b)

Type B tips are characterised by a zone of horizontal dilation of pre-existing joints which could be described as a tensile 'process zone' surrounding the tip. Close to the lateral tip, the fault plane generally passes laterally into a vertical ground 'fissure'. Fissures are crevasse-like structures with a downward narrowing cross section (maximum aperture at the surface), which penetrate to depths of 50 m or more as open extensional fractures. They can have both horizontal and vertical components of displacement, the relative magnitude of which depends on

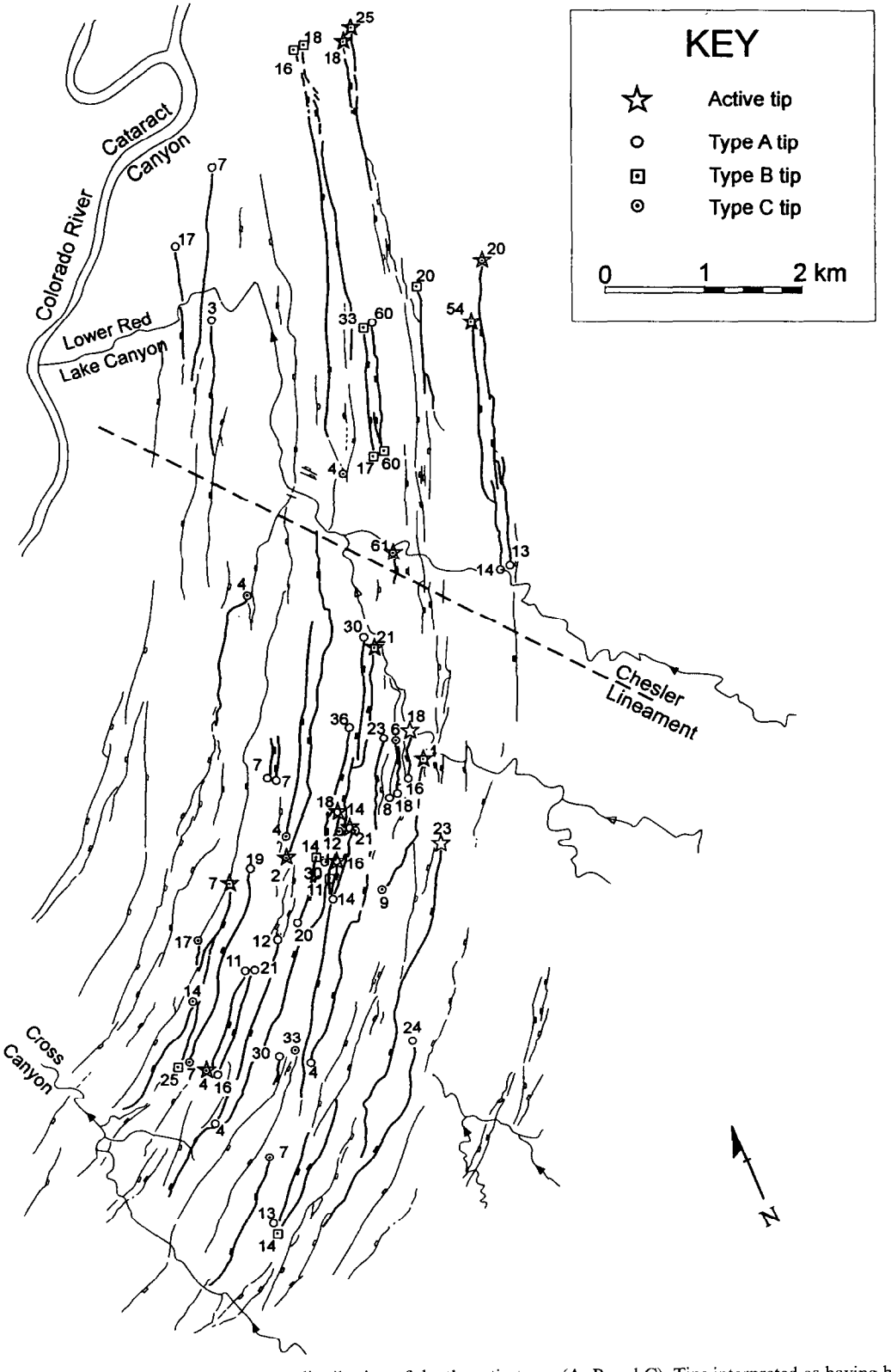

Fig. 5. Map of the study area showing the distribution of the three tip types (A, B and C). Tips interpreted as having been recently active are shown with a star symbol. The numbers are reciprocal values of lateral tip displacement gradients calculated using the first point method.

the position with respect to the fault tip. Beyond the tip, the main fault plane fissure usually links into a series of smaller vertical fissures via networks of extensionally-reactivated joints or, more rarely, newly formed fracture surfaces. The linked network of minor fissures is in most cases preferentially distributed in the region beyond the tip on the footwall side of the main fault, but the reason for this is not known.

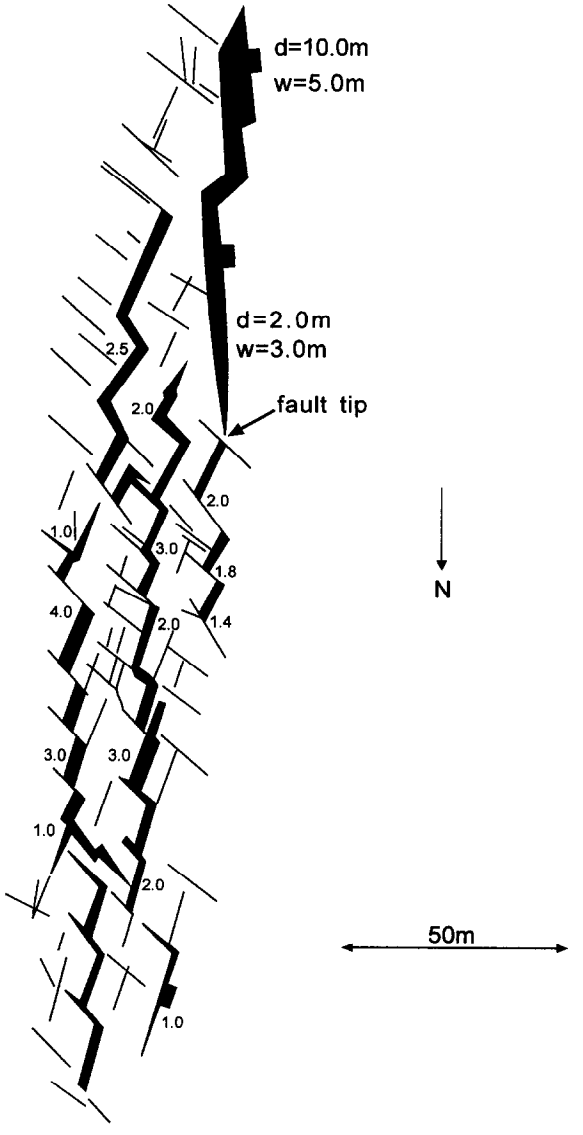

Fig. 6. Structural map of the NE tip of Fault 11 (located on Fig. 1). Shear offset on the main fault passes laterally into a zone of extensional fractures (fissures) on the footwall side ahead of the main fault tip. Solid black infill is used to represent schematically the amount of dilation of preexisting joints (thin lines). Small numbers refer to maximum width of fissures (also labelled w). Values of vertical displacement on the main fault are labelled, d.

A representative structural map of a Type B tip is presented in Fig. 6. Two preexisting joint sets occur in this area, oriented N040° and N135°. The vertical displacement on the main fault decreases from 10 m to zero over a distance of 100 m. This is accompanied by a corresponding decrease in the horizontal component of displacement, i.e. in the width of the fissure on the main fault. A region of 150 m by 50 m on the footwall margin ahead of the main fault tip is permeated with a network of minor fissures, typically with apertures at surface of less than 3 m. Most of the fissures opened by pure extensional reactivation of the N040° joint set, left-stepping along joints of the N135° set. The stepping sense of the fissures preserves the *ca* N020° strike of the main fault, whilst fully exploiting those joints oriented favourably for reactivation as extension fractures (c.f. McGill and Stromquist, 1979).

Type C tips (Fig. 4c)

This type of tip is characterised by a transition from a purely 'brittle' expression of the normal fault as a structure with vertical displacement of bedding across the fault plane with little or no normal drag, to a more 'ductile' expression of vertical displacement in the form of a monocline. As the vertical displacement across a fault decreases towards the tip point (zero throw on the fault), the amplitude of the monocline increases, but beyond the tip point, the amplitude progressively decreases to zero.

Dips of the steepest part of the monoclines vary along their fold axes, with the maximum bedding dip usually occurring close to the 'brittle' tip. Steep dips (> 45°) are common, with a maximum dip in the study area of 60° recorded at the SW tip of fault 8. Strike of bedding is closely parallel to the fault strike away from the tip, but closer to the tip region at the nose of the monocline, bedding strike often becomes almost orthogonal to fault strike.

A structural map of a Type C tip is presented in Fig. 7. The main fault trace has a serrated pattern, resulting from the reactivation of three joint sets. The displacement gradient (change in vertical displacement/distance) is *ca* 0.03, but reaches a local maximum of *ca* 0.04 in the sector where the fold amplitude decreases from 4.0 to 2.0 m. This part of the monocline is the most intensely fractured. The fractures associated with the development of the monocline consist entirely of extensionally reactivated joints. The width of the monocline as measured from the upper to the lower hinge is approximately constant, a feature that is typical of the all the Type C tips in the study area.

Evidence for recent activity

Fourteen out of the total of 73 mapped tips exhibit features consistent with recent fault activity (Fig. 5). Recent faulting in this context means within the past 50–100 years. The evidence for recent activity is the disruption of the soil profile by a fracture or fault, with exposure of live tree and shrub roots into voids (Fig. 8a). The slip on the fracture in these cases must have post-dated the growth of the disrupted shrubs. These have not been dated, but most are probably less than 100 years old. Other indications of relatively recent fault activity include sink holes developed directly above extensional fractures, and collapse of soils into graben-like depressions along extensional fractures. In some cases, the collapsed soil profile has preserved its integrity even though it has dropped vertically 5–10 m (Fig. 8b). This suggests strongly that soil collapse occurred in a single slip event. Local people have reported instances of ground tremors in the area this century (McGill and

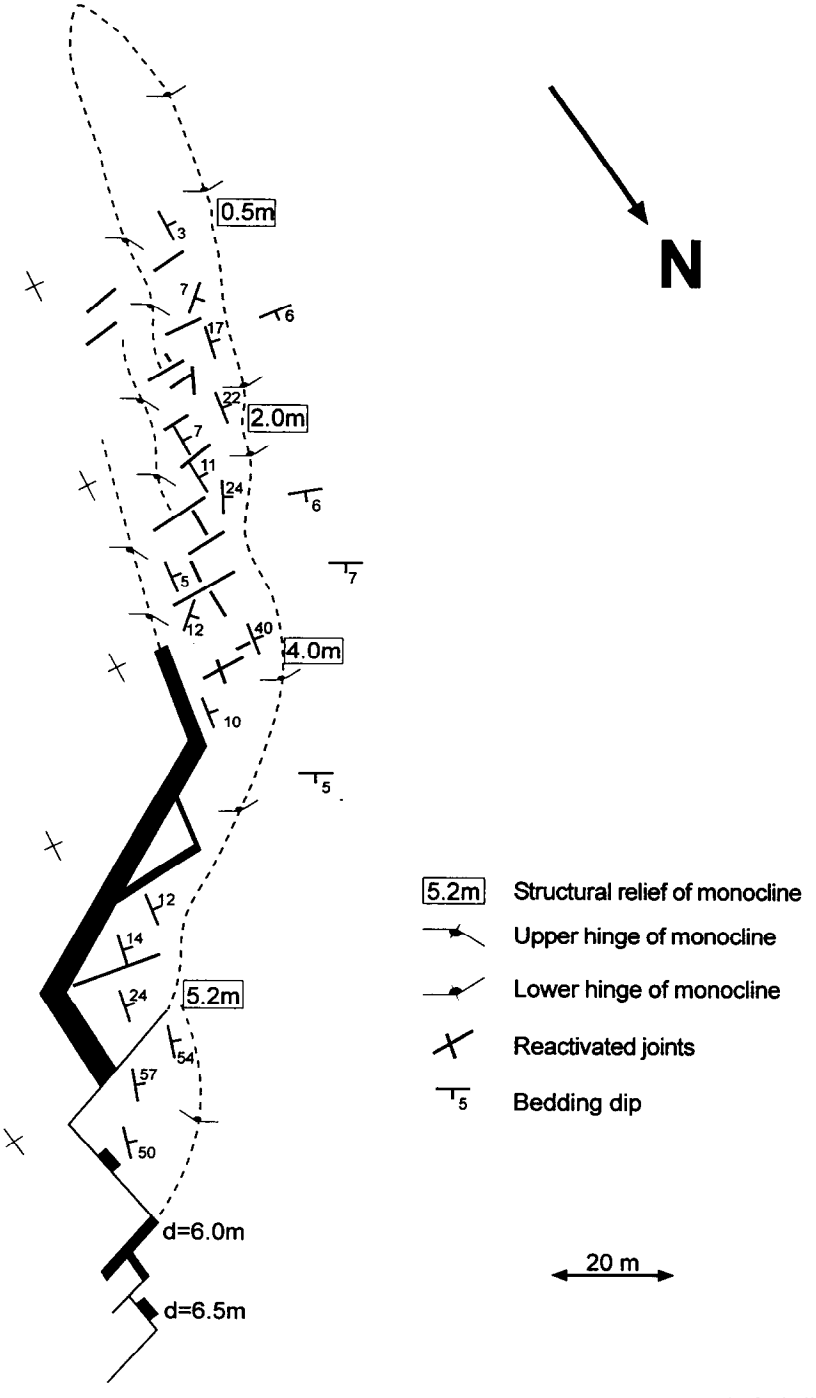

Fig. 7. Structural map of the Type C tip of Fault 17 (located on Fig. 1). As displacement across the fault dies out, the structural relief from footwall to hangingwall is expressed in a simple monocline, whose amplitude progressively reduces along strike to zero. The main crestal fissure system developed along the monoclinal crest is shown in solid black. d = amount of shear offset on the main fault surface.

Stromquist, 1979), and it is possible that some of the 'single slip' soil collapse structures were formed on these occasions.

Twelve out of the 14 recently active tips are located at the northern tips of their respective fault traces. Of the 14 recently active tips, five are type A, six are type B, and three are type C tips. Those faults with recently active tips only have one 'active' tip, i.e. these faults appear to be propagating asymmetrically (Fig. 5). The distribution of recently active tips is non-uniform: there is a clustering of recent activity in the central part of the study area, and on the most northeasterly tips in the region.

DISPLACEMENT VARIATION TOWARDS LATERAL TIPS

This section addresses the way in which displacement

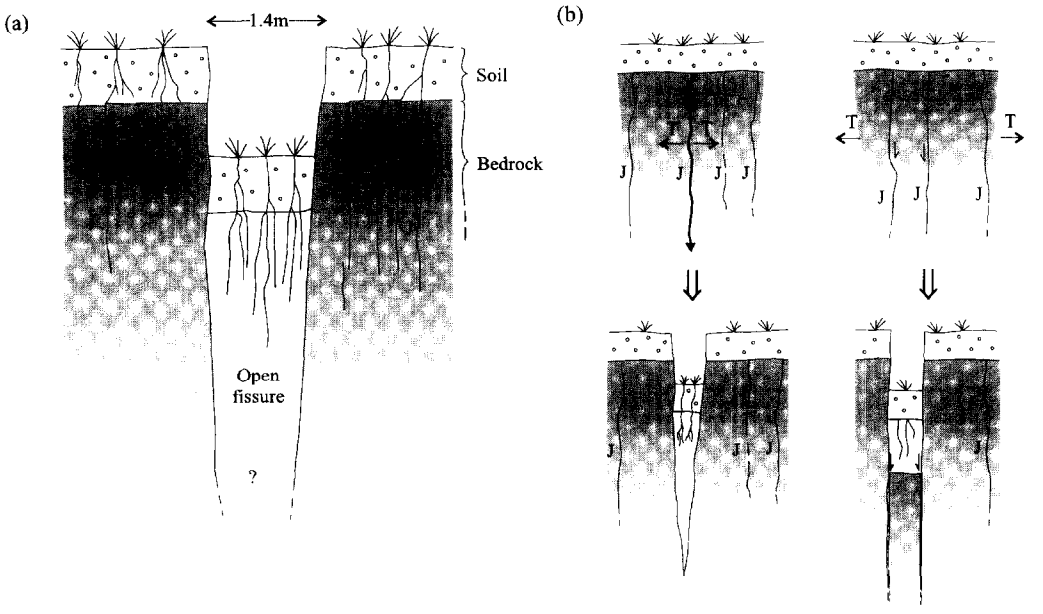

Fig. 8. (A) Schematic field sketch of surface features interpreted to have formed by recent extensional rupturing. (B) The full vertical extent and cross-sectional profile of the fissures is not known, so two possible geometries are presented. Tensile reactivation of either a single joint or pair of joints produces a downward tapering fissure or a parallel-sided fissure, respectively. Intact soil profiles in the collapsed block suggest that this occurred in a single slip event.

decreases on faults as the lateral tips are approached. Several previous workers have emphasised the importance of characterising lateral variations of displacement as an important step in developing physical models for fault growth (Cowie and Scholz, 1992a; Scholz *et al.*, 1993; Peacock and Sanderson, 1996). We begin by discussing the suitability of various strategies for characterising the observed variation on individual faults such that correlations can be attempted between displacement variation characteristics and various fault parameters (length, maximum displacement, etc).

Methodology

A major problem confronting any attempt to characterise lateral displacement variation towards the tips is to assess the shape of the displacement profile. Various idealised profiles have been discussed previously, from elliptical types (Walsh and Watterson, 1987, 1989) to those with linear displacement tapers ('C' or 'M' type profiles, Peacock and Sanderson, 1991). In such idealised cases, it would be feasible to use a curve-fitting approach and then use the parameters of the matched curve as a basis for comparison. Another approach might simply be to compile local displacement gradient values between adjoining measured values of displacement (Walsh and Watterson, 1989), and then compare the distribution of the 'local' gradients.

The problem presented by the displacement profiles shown in Fig. 3 is that they are so irregular and segmented, that they defy any simple categorisation based on overall form. Curve fitting was rejected simply because of this lack of systematic form to the lateral variation, with too many local maxima and minima. Similarly, the lack of consistency in the spacing of data points means that a method based on local gradient would be subject to smoothing errors due to variable distance over which the gradients were calculated, and so this approach was also rejected.

For the purely comparative purposes intended in this study, the most important requirements for the characterisation were that the same approach could be used on all the faults in the area with consistent and objective criteria. We considered using some arbitrary percentage of trace length over which to calculate an average gradient (P. Cowie, personal communication). This method was rejected because it would have led to the incorporation of gradient reversals in the overall displacement taper into the average value. This problem of potential gradient reversals stems from the variable length distribution of fault segments, and the asymmetry of many of the 'whole fault' displacement profiles. We instead considered approaches that were based on average values to systematically identifiable points on any fault. Four such methods were evaluated, shown diagrammatically in Fig. 9:

(1) The 'D_{max}' value is the lateral displacement gradient measured from the position of the maximum displacement value for the whole fault, to the lateral tip. This value is equivalent to the r/D_{max} value (r is the fault radius) widely used in fault analysis (e.g. the 'gross' displacement gradient value related to material shear modulus by Walsh and Watterson, 1989). The 'D_{max}' method was rejected because it does not take account of

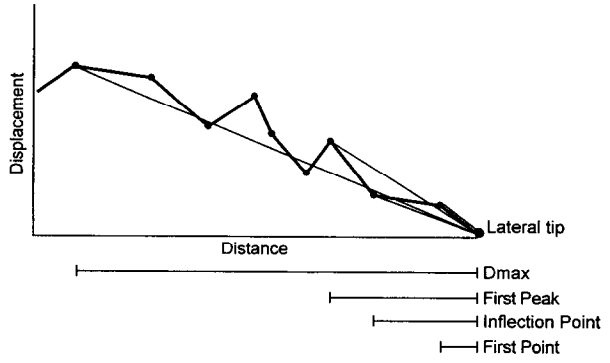

Fig. 9. Contrasting methods for measuring lateral displacement gradients of the tip regions of normal faults in the Canyonlands (from Mansfield, 1996).

the local displacement maxima and minima along the fault trace that relate to the numerous relay structures developed on most of the segmented faults;

(2) The 'First Maximum' value is the lateral displacement gradient from the tip to the first maximum displacement value recorded along any given fault. To qualify as a maximum, the deviation of the peak value above a smoothed trend (best fit curve) must be greater than the measurement error (maximum of 10%). First maximum positions corresponded in all cases to the sites of maximum displacement of the outer segments of the 20 fully surveyed faults. This method was selected partly because of the reliability with which the first maximum position could be located, and partly because of the potential significance of the displacement distribution on the outermost segment;

(3) The 'Inflection Point' value is the lateral displacement gradient measured from the tip to the nearest inflection point to the tip, taking into account a 10% error in displacement values. This type of value was considered because of the emphasis placed by Cowie and Scholz (1992a) on bell-shaped displacement profiles in their physical model of fault growth. However, unambiguous inflection points were only identified on a few of the faults in the study area (e.g. faults 36 and 220), so this method was rejected;

(4) The 'First Point' value is the lateral displacement gradient measured from the nearest displacement data point to the tip. As noted earlier, this first measurement point was selected specifically during displacement surveying on the basis of recognition of a linearly tapering displacement from that point to the tip. It is, however, subject to errors relating to the concealment of hangingwall bedrock topography (Fig. 2), but these values can be regarded as a close approximation ($\pm 10\%$) to the true value of lateral gradient. Significantly non-linear displacement tapers are not likely to be concealed by measurement 'noise' or surficial sedimentary cover. In a few cases, fault-parallel stream sections expose bedrock in the hangingwall near fault tips, and direct confirmation of linear tapers was made. A major limitation of this method is that the first point position was often located within 100 m of the tip, and for the larger faults this represents a small fraction ($< 10\%$) of the trace length. This method was selected, in spite of this limitation, to enable the significance of the linear taper to be evaluated further.

Results

First point and first maximum values of average lateral displacement gradients were obtained for 39 tips. These data are shown in a combined histogram form in Fig. 10, subdivided according to tip geometry. The data exhibit a range of over an order of magnitude from 0.0164 to 0.25.

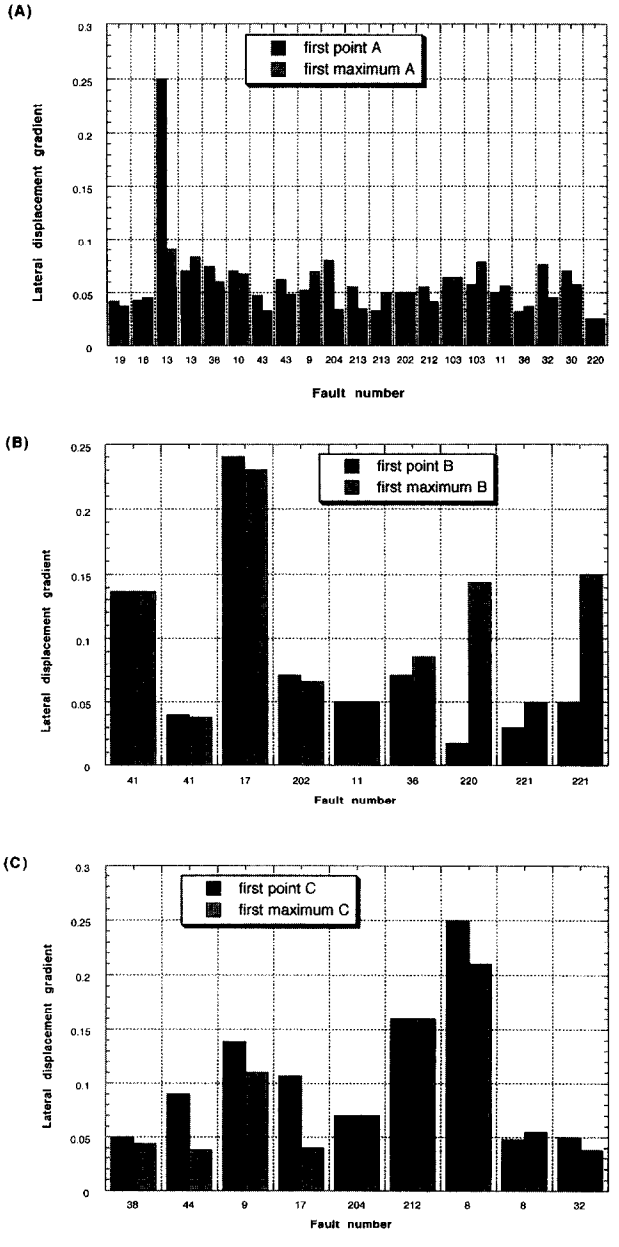

Fig. 10. Paired histograms (first point and first maximum methods) of average lateral displacement gradients separated according to tip type (A, B, C). The histograms are displayed by fault number to allow reference to Figs 1 & 5.

Comparable ranges of values are evident for the three tip types using either of the two methods. First point and first maximum values for individual tips are neither consistently larger nor smaller than one another. There is less than a 20% difference in the first point and first maximum values in 27 out of the 39 tips. This similarity is another indication of the almost linear tapering of displacement from first maximum positions to the tips in many of the fault profiles.

The means and standard deviations for the first point method for the three types of tip are 0.065 and 0.045 (Type A), 0.078 and 0.07 (Type B), and 0.107 and 0.067 (Type C). Means and standard deviations for the first maximum method are 0.052 and 0.017 (Type A), 0.106 and 0.063 (Type B), and 0.085 and 0.062 (Type C). Tips classified as being recently active (Fig. 5) exhibit a similar range of lateral displacement gradients to the remainder of the tip dataset (range from 0.0164 to 0.25, mean value of 0.099, standard deviation of 0.097). The mean value for the combined dataset (A, B, C) is 0.078 (first point) and 0.072 (first maximum), with standard deviations of 0.058 and 0.049, respectively.

Lateral displacement gradients measured using the two methods were plotted against a number of fault parameters including fault trace length, maximum displacement, maximum displacement/fault length, distance to nearest fault, segment length (of the outermost segment), and maximum displacement/segment length, but no positive correlations were found for any of these combinations. A selection of these graphs is shown in Fig. 11. It is evident from the lack of correlation with fault length and segment length, that the variation in lateral displacement gradients is not related to fault dimensions in any obvious way. A reference line for an isolated 'C' type displacement profile (Nicol *et al.*, 1996) is shown along with the Canyonlands data in Fig. 11(a), to emphasise the deviation of these data from idealised profile systematics.

In addition to trial correlations between fault or fault segment parameters and lateral displacement gradients, the data were analysed for any obvious geographic relationships, such as particular ranges of values in particular regions of the study area. Aside from the virtual absence of Type C tips north of the Chesler Lineament (Fig. 5) (see Discussion), no geographic biases in the data could be detected.

DISCUSSION

Tip geometry and propagation modes

The subdivision of the lateral tips in the study area into three geometrical classes is based primarily on the structural associations observed in the immediate region surrounding the tips, and is not a function of how rapidly displacement decreases as the tip is approached. Since the underlying aim of this paper is to investigate how displacement characteristics towards the lateral tips might provide insights about lateral fault propagation processes, it is pertinent to discuss the mechanical significance of the three-fold tip sub-division.

By analogy with terminology applied in fracture mechanics to describe different modes of fracture (Atkinson, 1987), Type A tips (Fig. 4a) are considered to exhibit Mode III geometry with a torsional offset of footwall and hangingwall strata. This displacement geometry suggests that lateral propagation could have been driven by Mode III loading conditions, assuming the analogy with fracture mechanics can be scaled up to apply to large normal faults (Atkinson, 1987; Cowie and Scholz, 1992a). Uncertainty in the mechanical significance of this type of tip, however, arises from the lack of significant process zones in the tip regions (c.f. McGrath and Davison, 1995). Complete exposure of bedrock around the tips is rarely seen, so minor fractures that could be indicative of specific failure conditions around the tip region may be concealed under the soil cover.

The decay of the fault-parallel component of displacement (vertical component in most cases) towards Type B tips is also typical of a Mode III geometry, but the important distinction between Types A and B, is that Type B tips are characterised by a tensile 'process zone.' This often elongate zone with a long axis parallel or subparallel to the strike of the fault, and consisting of a network of extensional fractures, must represent failure under Mode I loading conditions. This inference is reasonable given the fact that propagation occurs at the free surface under low values of vertical effective stress. The most important observation regarding Type B tips is that normal faults with only a shear component of displacement (near-vertical displacement vector at surface) pass laterally into 'fissures' with combined shear and dilational components (vertical and horizontal displacement vectors), that gradually lose the vertical component whilst the horizontal component increases, until beyond the tip, only the horizontal component remains (e.g. main fault on Fig. 6).

This transition from a fault plane with a 'Mode III' geometry into a zone of distributed Mode I fractures is similar to the structure of lateral tips of normal faults described by Peacock and Sanderson (1992) and by McGrath and Davison (1995) in the Lower Jurassic of Somerset, England, and to the lateral tips of some Icelandic normal faults described by Gudmundsson (1987a). The similarity between the Icelandic and Canyonlands faults is particularly relevant, since the faults are similar in scale, and in both cases surface fissures are developed along portions of the normal faults. Gudmundsson (1987a,b) proposed that normal faults in Iceland develop by firstly propagating as pure extensional fractures and subsequently maturing into normal faults through accumulation of a shear component of displacement once the vertical extensional fractures propagate downwards to some critical depth. Cartwright *et al.* (1995, 1996) have also argued for initial

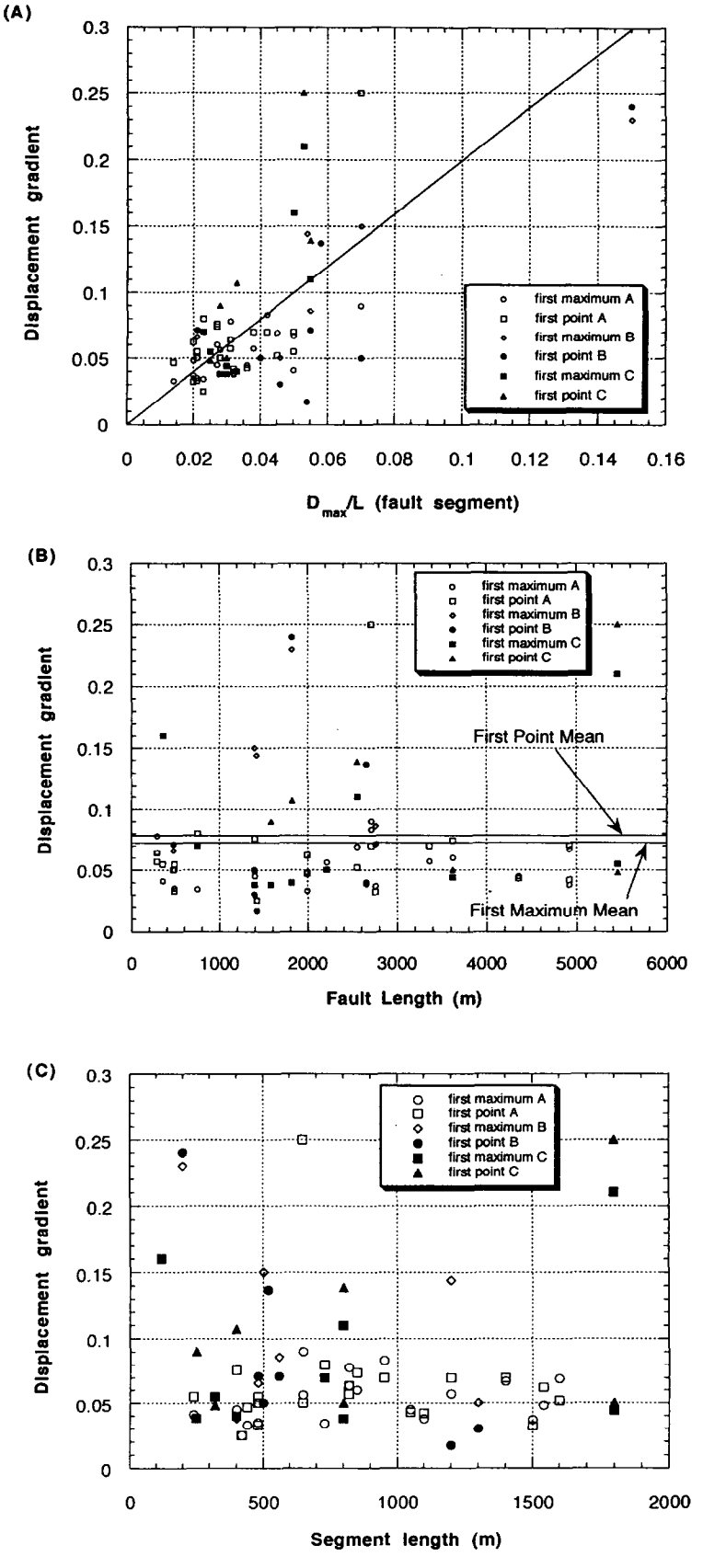

Fig. 11. Cross-plots of average lateral tip displacement gradients (three tip types separated for the two methods) with (A) maximum displacement of the whole fault/trace length, (B) fault length, and (C) segment length. No positive correlations are evident for any of these plots. In (A), a reference line is drawn based on the ideal 'C' type displacement profile (Nicol *et al.*, 1996). In (B), the horizontal lines are mean values of average lateral displacement gradients for all tip types for the two methods.

nucleation at the surface followed by downward and lateral propagation as subsequent displacement accumulates, and it seems reasonable, therefore, to draw a close analogy between the propagation history of faults in the two areas in spite of their contrasting tectonic settings.

The growth history envisaged to explain Type B tips is illustrated in Fig. 12. Initial propagation is from the free surface downwards as a Mode I extensional 'fissure' with purely horizontal displacement. The region beyond the main fissure is shown to be the locus for a set of subparallel minor extensional 'fissures'. These minor 'fissures' are the precursors for the main 'fissure'. At some limiting depth, failure in tension is no longer possible due to increasing overburden stresses (Gudmundsson, 1987b), and further radial propagation occurs as increments of shear displacement accumulate. In this propagation model, Type B tips can be visualised to be an expression of lateral propagation under the stage (i) Mode I loading configuration, with the Mode III displacement geometry being the result of the lateral tapering in the fault-parallel component of displacement. In this situation it could be feasible to distinguish two tiplines, associated with the zero values of fault-parallel and fault-normal components of displacement, respectively.

Type C tips correspond closely to the ductile drag geometry described by Walsh and Watterson (1987), which they interpreted as resulting from lateral propagation of normal faults into a 'precursory monocline'. This type of lateral tip geometry has been recognised in many areas of normal faulting (e.g. Huggins *et al.*, 1995), and similar structures were recognised by Elliott (1976) at the lateral tips of thrust faults. Elliott (1976) interpreted these tip folds as a form of 'ductile bead' that developed ahead of the propagating brittle structure. The restriction of monoclinal 'drag' structures in many faults in the Canyonlands to the lateral tips regions strongly suggests that Type C tips are a specific variant of a Mode III tipline, differing from Type A tips in their partitioning of the displacement into a brittle and ductile component, with the 'ductile' yielding zone preceding the development of the through-going fault plane. No firm explanation can currently be offered, however, as to why displacement is partitioned in this way in some cases and not in others. In the absence of any field evidence linking Type C tips to specific rock types (and rheology), we can only speculate that it is somehow connected with the rate of lateral propagation, with the more ductile yielding behaviour being characteristic perhaps of a prolonged period of locking of the tip.

Distribution of tip types

It can be seen in Fig. 5 that there is no systematic distribution of tip types on individual faults. Also, there is no correlation between specific tip types and fault parameters (Fig. 11). The lack of correlation of tip type with length is interesting since it implies that the tip geometry is not a function of whether a specific fault is restricted in extent to the post-salt units, or whether it soles into the salt units of the Paradox Formation. Faults of trace lengths less than 400–500 m (the post-salt stratigraphic thickness) could be expected to be confined within the 'brittle' post-salt section, but they have the same combination of tip types as much longer faults (Fig. 5).

It was noted earlier that the only recognisable bias in geographic distribution of the tip types was that Type C tips were relatively rare in the region north of the Chesler Lineament (Fig. 5). The surface rocks exposed in this northern region are the thick aeolian beds of the Cedar Mesa Formation (Lewis and Campbell, 1965), and these

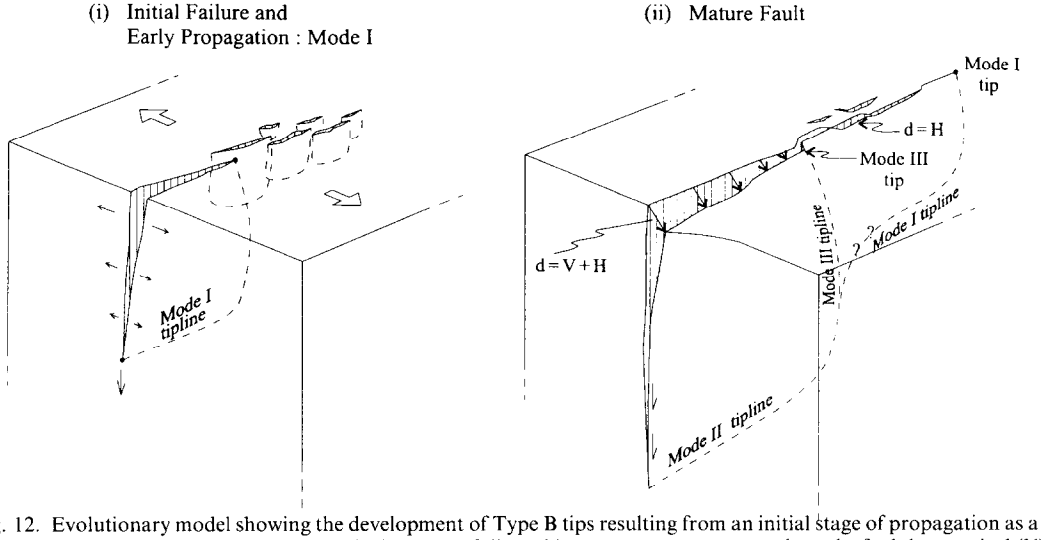

Fig. 12. Evolutionary model showing the development of Type B tips resulting from an initial stage of propagation as a pure extensional fracture with only horizontal displacement, followed by a more mature stage where the fault has vertical (V) and horizontal (H) components of displacement (c.f. Gudmundsson, 1987a). Different tipline modes are shown, based on the displacement geometry relative to the possible tipline configuration.

are intensely fractured by deeply penetrating (up to 100 m) vertical joints oriented N030° (McGill and Stromquist, 1979). The rarity of Type C tips in this area is most easily explained by the presence of this dominant joint set, and its influence on folding. Thick-bedded units with closely-spaced, deeply penetrating, vertical joints are not as likely to bend into tight monoclines as easily as thin-bedded units with smaller joints. This explanation points to a link between tip geometry and those material parameters such as bulk strength and shear modulus that would be affected by the dimensions and orientations of joint sets. However, it does not imply that the origin of Type C tips is controlled by rock rheology (see previous section).

Lateral displacement variation

Two aspects of the displacement profiling results are most relevant to the theme of fault growth. Firstly, the recognition of linear displacement tapers towards the lateral tips, and secondly, the range of over an order of magnitude in lateral displacement gradients for all three tip types and for those tips deemed to be recently active (Figs 5 & 10). The other notable feature is the irregularity of the displacement profiles. This irregularity is attributable to segment linkage, and these Canyonlands examples therefore merely substantiate well established principles regarding interaction of overlapping segments during linkage developed by Walsh and Watterson (1990) and Peacock and Sanderson (1991), and given a physical basis by Burgmann *et al.* (1994) and Willemse *et al.* (1996).

The post-yield fracture mechanics model for faults developed by Cowie and Scholz (1992a) predicted that the lateral displacement taper would be bell-shaped, with a process zone developed at the tip, where the peak stress is just equal to the shear strength of the surrounding rock. Bell-shaped profiles of the type described by Cowie and Scholz (1992a) have not been recognised as a general characteristic for Canyonlands faults, although several faults have gentle inflections at some position between the first maximum and the tip (e.g. faults 36, 38 and 220; Fig. 3). Instead, the most common form of lateral displacement decay for the surveyed faults is a linear taper, particularly in the zone adjacent to the tips, i.e. within a distance of approximately 10% of the trace length.

Linear displacement tapering towards lateral tips has also been recognised by Cowie and Shipton (submitted), for a fault in SE Utah, using much higher resolution displacement techniques than those described in this paper. To explain the linear taper, Cowie and Shipton (submitted) have proposed a fault growth model involving positive feedback between rupture and reloading of a fault as it accumulates displacement. One of the main differences between this physical model and previous models is that the fault is considered to rupture in slip patches due to strength heterogeneities that are small relative to fault dimensions. Their numerical modelling shows that a linear taper results when the slipping patch is much smaller than the fault dimensions, and strength recovery is instantaneous.

This model is appealing as an explanation for the linear displacement tapers observed in the Canyonlands, in that the length scale of the main strength heterogeneities in the sedimentary rocks of the post-salt section is dictated by the joint dimensions and these are much smaller (1–200 m length) than the typical fault dimensions mapped at the present day (150–6000 m).

The range of lateral displacement gradients presented in Fig. 10 is larger than might be expected for faults propagating in a layer-cake stratigraphic sequence in a single deformational phase with simple mechanical boundary conditions. The similarity in the ranges of the recently active faults with the remainder of the tips is particularly intriguing. This suggests that attempts at lateral propagation are not restricted to faults whose lateral displacement tapers satisfy a single critical value of shear strain that equates to a local scaling condition for fault growth.

Some of the variation in lateral displacement gradients is attributable to interaction effects (Peacock and Sanderson, 1991; Burgmann *et al.*, 1994; Willemse *et al.*, 1996), although it must be noted that the evidence for these effects is restricted to observations based on two-dimensional (surface) exposure. Nevertheless, the asymmetry of some of the whole-fault displacement profiles (as opposed to segment profiles) such as fault 8, is most easily explained by interactions with nearest neighbours in overlapping configurations. However, the asymmetry of displacement distribution on some relatively isolated faults (e.g. faults 220 and 221) is less easily explained by interaction. Other possible explanations for contrasting displacement gradients at either ends of relatively isolated faults in the Canyonlands include variations in rock strength, possibly related to lateral variability in joint dimensions, spacing and orientation (Mansfield, 1996), or more speculatively, variations in frictional properties of the fault surfaces and/or spatial gradients in the stress field (Burgmann *et al.*, 1994). These latter two possibilities are extremely difficult to quantify, although we have observed significant variations in fault zone microstructure and composition (unpublished field data) that would support the notion of lateral variability in frictional strength of the faults.

In addition to the factors listed above, an important factor that could have influenced the range in tip gradients is the linkage 'state'. By this we mean the timing of linkage at the various relay structures along any particular segmented fault, and the magnitude and distribution of post-linkage displacement addition. If fault growth is governed by some form of scaling relationship between displacement and length as is widely believed to be the case (Walsh and Watterson, 1988; Cowie and Scholz, 1992b; Gillespie *et al.*, 1992; Scholz *et al.*, 1993; Schlische *et al.*, 1996), then the process

of lateral segment linkage is likely to distort the balance between addition of length and displacement, and result in temporary deviation from idealised scaling behaviour (Cartwright *et al.*, 1995). For faults that undergo multiple lateral linkages resulting in multifold increases in length, if there is insufficient time between linkages to return to the idealised growth path, the fault may be 'under-displaced', i.e. have too little accumulated displacement for its new length (Cartwright *et al.*, 1996). In such a case, it should be expected that the lateral displacement tapers would be lower than required for continued lateral propagation of the newly lengthened fault. Segment linkage, particularly where more than one relay structure is involved, may thus contribute to the observed range in lateral displacement gradients.

An underlying theme of this paper has been to emphasise the variability in fault displacement distributions mappable from a well exposed fault array. Numerical or analogue-based studies of fault behaviour necessarily simplify variables such as material properties and mechanical boundary conditions, and tend to emphasise aspects of fault behaviour that conform to well-defined relationships that have predictive implications (e.g. length vs displacement scaling). The complexity of the displacement field described here, in what is essentially a simple, single-phase deformational province composed of relatively uniform rock types, and the difficulty encountered in attempting to explain the variations in displacement in terms of the possible contributory factors are cautionary notes that are worth further consideration when attempting extrapolations of resolution-limited fault maps using sub-surface datasets.

CONCLUSIONS

Displacement distributions of 20 normal faults surveyed in the Canyonlands exhibit considerable variation, with generally irregular profiles related to fault segmentation. Whole-fault profiles range from symmetric to asymmetric in shape. Some of the asymmetric profiles are related to fault interaction similar to that interpreted for asymmetric profiles of individual segments. Three types of tip geometry are distinguished on the basis of contrasting minor structures developed in the tip regions. No systematic distribution of these three types of tip is apparent either on individual faults or throughout the study area. Lateral displacement gradients defined with two alternative approaches for 39 tips exhibit over an order of magnitude range. A similar range is exhibited by tips interpreted to have been recently active, suggesting that this range is representative of dynamic fault growth processes. No significant differences in displacement gradient could be detected for the three tip types, and displacement gradients do not correlate positively with any measured fault parameters (length, maximum displacement, fault spacing, etc). This lack of correlation is consistent with theoretical models showing that displacement distribution is influenced by factors including interaction, strength heterogeneities, frictional properties of the fault surfaces, and linkage history. The complexities of the displacement distribution exhibited in the Canyonlands fault system provide a cautionary example for the extrapolation and correlation of faults in sub-surface mapping, where the primary data (e.g. seismic) has limited resolution of fault displacement.

Acknowledgements—Shell Research B.V. (JAC), Shell UK Ltd. (CM), Fina UK Ltd. and the Nuffield Foundation (JAC) are thanked for their financial support of this research. We are also indebted to the National Park Service in Moab and at the Needles District Station for much valuable assistance with logistics. Patience Cowie is thanked for valuable discussions, and Jim Evans, David Peacock and an anonymous referee are thanked for their insightful reviews of the manuscript.

REFERENCES

Atkinson, B. K. (1987) *Fracture Mechanics of Rocks*. Academic Press Geology Series. Academic Press, London.

Baker, A. A. (1933) Geology and oil possibilities of the Moab district, Grand and San Juan counties, Utah. *U.S. Geological Survey Bulletin* **841**, 95.

Burgmann, R., Pollard, D. D. and Martel, S. J. (1994) Slip distributions on faults: effects of stress gradients, inelastic deformation, heterogeneous host-rock stiffness, and fault interaction. *Journal of Structural Geology* **16**, 1675–1690.

Cartwright, J. A., Trudgill, B. D. and Mansfield, C. S. (1995) Fault growth by segment linkage: an explanation for scatter in maximum displacement and trace length data from the Canyonlands Grabens of SE Utah. *Journal of Structural Geology* **17**, 1319–1326.

Cartwright, J. A., Mansfield, C. S. and Trudgill, B. D. 1996. Fault growth by segment linkage. In *Modern developments its structural interpretation*, eds P. C. Buchanan and D. A. Nieuwland, Vol. 99, pp. 163–177. *Special Publication of the Geological Society of London.*

Cowie, P. A. and Scholz, C. H. (1992) Physical explanation for the displacement–length relationship of faults using a post-yield fracture mechanics model. *Journal of Structural Geology* **14**, 1133–1148.

Cowie, P. A. and Scholz, C. H. (1992) Displacement–length scaling relationship for faults: data synthesis and discussion. *Journal of Structural Geology* **14**, 1149–1156.

Cowie, P. A. and Shipton, Z. Quasistatic fault slip as an explanation for finite displacement gradients at fault tips. *Submitted to Journal of Structural Geology.*

Dawers, N. H., Anders, M. H. and Scholz, C. H. (1993) Growth of normal faults: Displacement–length scaling. *Geology* **21**, 1107–1110.

Dawers, N. H. and Anders, M. H. (1995) Displacement–length scaling and fault linkage. *Journal of Structural Geology* **17**, 607–614.

Elliott, D. (1976) Energy balance and deformation mechanisms of thrust sheets. *Philosophical Transactions of the Royal Society of London* **A283**, 289–312.

Gillespie, P. A., Walsh, J. J. and Watterson, J. (1992) Limitations of displacement and dimension data for single faults and the consequences for data analysis and interpretation. *Journal of Structural Geology*. **14**, 171–183.

Gudmundsson, A. (1987) Geometry, formation and development of tectonic fractures on the Reykjanes Peninsular, southwest Iceland. *Tectonophysics* **139**, 295–308.

Gudmundsson, A. (1987) Tectonics of the Thingvellir fissure swarm, SW Iceland. *Journal of Structural Geology* **9**, 61–69.

Hintze, L. F. (1988) Geologic history of Utah. *Brigham Young University Geology Studies Special Publication* **7**, 202.

Huggins, P., Watterson, J., Walsh, J. J. and Childs, C. (1995) Relay zone geometry and displacement transfer between normal faults recorded in coal mine plans. *Journal of Structural Geology* **17**, 1741–1755.

Lewis, R. Q. and Campbell, R. H. (1965) Geology and uranium deposits of Elk Ridge and vicinity, San Juan County, Utah. *U. S. Geological Survey Professional Paper* **351**, 68.

Mansfield, C. S. (1996) Fault growth by segment linkage. Unpublished Ph.D thesis, University of London.

McGill, G. E. and Stromquist, A. W. (1979) The grabens of Canyonlands National Park, Utah: Geometry, Mechanics and Kinematics. *Journal of Geophysical Research* **84**(B9), 4547–4563.

McGrath, A. G. and Davison, I. (1995) Damage zone geometry around fault tips. *Journal of Structural Geology* **17**, 1011–1024.

Nicol, A., Watterson, J., Walsh, J. J. and Childs, C. (1996) The shapes, major axis orientations and displacement patterns of fault surfaces. *Journal of Structural Geology* **18**, 235–248.

Peacock, D. C. P. and Sanderson, D. J. (1991) Displacements, segment linkage and relay ramps in normal fault zones. *Journal of Structural Geology* **13**, 721–733.

Peacock, D. C. P. and Sanderson, D. J. (1992) Effects of layering and anisotropy on fault geometry. *Journal of the Geological Society of London* **149**, 793–802.

Peacock, D. C. P. and Sanderson, D. J. (1996) Effects of propagation rate on displacement variations along faults. *Journal of Structural Geology* **18**, 311–320.

Schlische, R. W., Young, S. S., Ackermann, R. V. and Gupta, A. (1996) Geometry and scaling relationships of a population of very small rift-related normal faults. *Geology* **24**, 683–686.

Scholz, C. H., Dawers, N. H., Yu, J.-Z., Anders, M. H. and Cowie, P. A. (1993) Fault growth and fault scaling laws: Preliminary results. *Journal of Geophysical Research*, **98**, B12, 21, 951–21, 961.

Schultz, R. A. and Moore, J. M. (1996) New observations of grabons from the Needles District, Canyonlands National Park, Utah. In *Geology and Resources of the Paradox Basin*, eds. A. C., Huffman, W. R. Lund and L. H. Godwin, Vol. 25, pp. 295–302. *Utah Geological Association Guidebook.*

Trudgill, B. D. and Cartwright, J. A. (1994) Relay ramp forms and normal fault linkages — Canyonlands National Park, Utah. *Bulletin of the Geological Society of America* **106**, 1143–1157.

Walsh, J. J. and Watterson, J. (1987) Distributions of cumulative displacement and seismic slip on a single normal fault surface. *Journal of Structural Geology* **9**, 1039–1046.

Walsh, J. J. and Watterson, J. (1988) Analysis of the relationship between displacement and dimensions of faults. *Journal of Structural Geology* **10**, 239–247.

Walsh, J. J. and Watterson, J. (1989) Displacement gradients on fault surfaces. *Journal of Structural Geology* **11**, 307–316.

Walsh, J. J. and Watterson, J. (1990) New methods of fault projection for coalmine planning. *Proceedings of the Yorkshire Geological Society* **48**, 209–219.

Walsh, J. J. and Watterson, J. (1991) Geometric and kinematic coherence and scale effects in normal fault systems. In *The Geometry of Normal Faults*, eds A. M. Roberts, G. Yielding and B. Freeman, Vol. 56, pp. 193–203. *Special Publication of the Geological Society of London.*

Willemse, E. J. M., Pollard, D. D. and Aydin, A. (1996) Three-dimensional analyses of slip distributions on normal fault arrays with consequences for fault scaling. *Journal of Structural Geology* **18**, 295–309.